INDONESIAN JOURNAL ON GEOSCIENCE
Geological Agency
Ministry of Energy and Mineral Resources

Journal homepage: http://ijog.geologi.esdm.go.id
ISSN 2355-9314, e-ISSN 2355-9306

Mineralogical, Geochemical, and Raman Spectral Characteristics of Amphibole Mineral Types in Amphibolite from Southern Sanandaj-Sirjan Metamorphic Belt (Iran)

Hesam Moeinzadeh[1], Hadiseh Rahimisadegh[1], M. Moazzen[2], and K. Nakashima[3]

[1]Geology Department, Shahid Bahonar University of Kerman, Kerman, Iran
[2]Earth Science Department, University of Tabriz, 51666, Tabriz, Iran
[3]Earth and Environmental Science Department, University Yamagata, Yamagata990, Japan

Corresponding author: hadiseh.rahimi@sci.uk.ac.ir
Manuscript received: November, 07, 2018; revised: June, 18, 2019;
approved: June, 13, 2020; available online: February, 09, 2020

Abstract - The current study is related to amphiboles in amphibolite rocks in the northwest of Golgohar Iron Mine located in the southern part of Sanandaj-Sirjan metamorphic zone.Petrography observations indicate that the studied rocks are of ortho-amphibolite type, formed from metamorphism of igneous rocks. The analysis of amphibole crystals in amphibolites of the region was done by petrography, electron microprobe, and Raman spectroscopy. Raman spectral pattern of the studied minerals was discussed in comparison to mineral type and chemistry characteristics. Based on mineral chemistry studies, it was discovered that all amphiboles in the studied rocks are calcic with $(Ca+Na)_B \geq 1.34$ and Si^{IV} between 6.27 and 6.76 atoms per formula unit. Based on their enrichment in the elements Al and Fe^{3+}, their composition varies from tschermakite to magnesio-hornblende. Raman spectral peak pattern for amphiboles and terrestrial tremolite does not have significant discriminable differences. However, Raman peak patterns of tremolite have clearly different features versus tschermakite. According to the general formula of amphiboles $[A_{0-1}B_2C_5T_8O_{22}(OH, F, Cl)_2]$, the Raman spectrum variability of the tschermakite and tremolite can be due to the position of A site, Al incorporation into $M_1 + M_2 + M_3$ sites and into the T site.

Keywords: amphibole, electron microprobe, Raman Spectroscopy, Sanandaj-Sirjan metamorphosed zone, Golgohar Iron Mine

How to cite this article:
Rahimisadegh, H., Moeinzadeh, H., Moazzen, M., and Nakashima, K., 2021. Mineralogical, Geochemical, and Raman Spectral Characteristics of Amphibole Mineral Types in Amphibolite from Southern Sanandaj-Sirjan Metamorphic Belt (Iran). *Indonesian Journal on Geoscience*, 8 (1), p.59-72. DOI: 10.17014/ijog.8.1.59-72

Introduction

Background

Amphiboles ($A_{0-1}B_2C_5T_8O_{22}W_2$) are common rock-forming minerals that occur in wide geological and lithological ranges (Deer *et al.*, 1992). Amphibole group minerals occur in a great variety of igneous and metamorphic rocks with a wide range of pressure and temperature environments. A standard amphibole formula has the ideal form of $A_{0-1}B_2C_5T_8O_{22}(OH, F, Cl)_2$, where A= Na, K; B= Na, Li, Ca, Mn, Mg, Fe^{2+}; C= Mg, Fe^{2+}, Mn, Al, Fe^{3+}, Ti; and T=Si, Al. In general, depending on the complex nature of the amphibole structure, comparisons of amphibole compositions are carried out following the chemical analyses into the structural formulae (Hawthorne *et al.*,2012).

The International Mineralogical Association (IMA) amphibole nomenclature scheme (Leake, 1978; Rock and Leake, 1984), which is suitable for the classification of amphibole analysis both from electron-microprobe and wet-chemical analyses, was revised by the 1997 IMA report (Leake *et al*., 1997) and also by Hawthorne *et al*. (2012).

Mineral chemistry of amphibole can help us to understand the lithospheric processes (Tiepolo *et al*., 2007). Considering the capability of amphibole to accommodate a wide range of major and trace elements, its composition can be used to decipher physico-chemical conditions during magmatism and metamorphism (Anderson and Smith, 1995; Holland and Blundy, 1994).

In order to characterize the amphibole in the amphibolites from the NW of the Golgohar Iron Mine in the Sanandaj-Sirjan belt, electron probe microanalyses along with an investigation by Raman Spectroscopy were carried out. The results of these two methods are presented in this contribution.

A combined Raman spectroscopy and electron microprobe results provide a promising methodological approach to understand particular features of cation diffusion for fine-grained amphiboles during metamorphism, and is a useful method to discriminate fibrous minerals with similar structure and/or chemical composition.

In general, in the current work, two overall innovated aims are: i) for the first time, introducing typological and mineral chemistry properties of rock forming minerals in amphibolitic rocks from the southern part of Sanandaj-Sirjan metamorphic belt in northwest of Golgohar Iron Mine, and ii) introducing experimental functions between mineralogical and chemical characteristics and Raman spectral patterns of each introduced amphibole type in the studied area.

Geological Settings

Metamorphic rocks of northwest of Golgohar Iron Mine are located in the Sanandaj-Sirjan belt. This belt is situated at the south and southwest of Central Iran and northeast of Zagros orogen (Figure 1). Structure of Sanandaj-Sirjan belt is controlled by opening and later closure of Neotethys at the southeastern margin of Gondwana (Alavi, 1994). The main structure of the Sanandaj-Sirjan belt can be summarized in three main events including northeastward subducting of the Arabian Plate beneath the Central Iranian Plate, the formation of coloured mélange of Sanandaj-Sirjan belt, and finally the continental collision between two plates in Miocene.The most important rifting phase in the Zagros Basin started apparently during Permian (Ricou, 1994; Mehdipour Ghazi and Moazzen, 2015). This phase was preceded by a wide regional pre-Permian erosion on both shoulders of the rift (Sanandaj-Sirjan Zone and Arabian Plate Margin) indicated by Ordovician-Carboniferous sediments missing in the Sanandaj-Sirjan Zone and most other parts of Iran, which is attributed to epeirogenic movements associated with the Caledonian and Hercynian orogenies in Europe and Northwest Africa (Stöcklin, 1968; Berberian and King, 1981; Aghanabati, 2006). This was followed by major asymmetric mafic (basalt, diabase, and some intermediate) volcanic activity in the Late Permian along the Sanandaj-Sirjan Zone. Neotethys began opening between a lower plate in Arabia and the Sanandaj-Sirjan Zone on the upper plate in Permian. By Late Permian, Neotethyan simple shear rifting had affected the whole length of the present-day Zagros orogen (Mohajjel and Fergusson, 2000). A second rifting phase started along the South Sanandaj-Sirjan Zone during Triassic times.

The oldest rock units of Triassic to Early Paleozoic at northwest of Golgohar Iron Mine include amphibolite, biotite amphibolite, garnet-staurolite schist, garnet schist, and lower grade amphibole schist, biotite schist, greenschist, gneiss, and metabasalts which are covered by a sequence of younger marble, quartzite, and non-metamorphic rocks such as mudstone, limestone, and calcareous sandstones(Figure 1).

The mafic rocks have changed to greenschist and amphibolite due to multiple phases of metamorphism. Amphibolites are exposed in the central and southern parts of the studied area. These rocks are dark green in colour and show clear lineation as a result of deformation. They are crashed in some places owing to activities in the shear zones. Isoclinal microfolds are developed in amphibolites

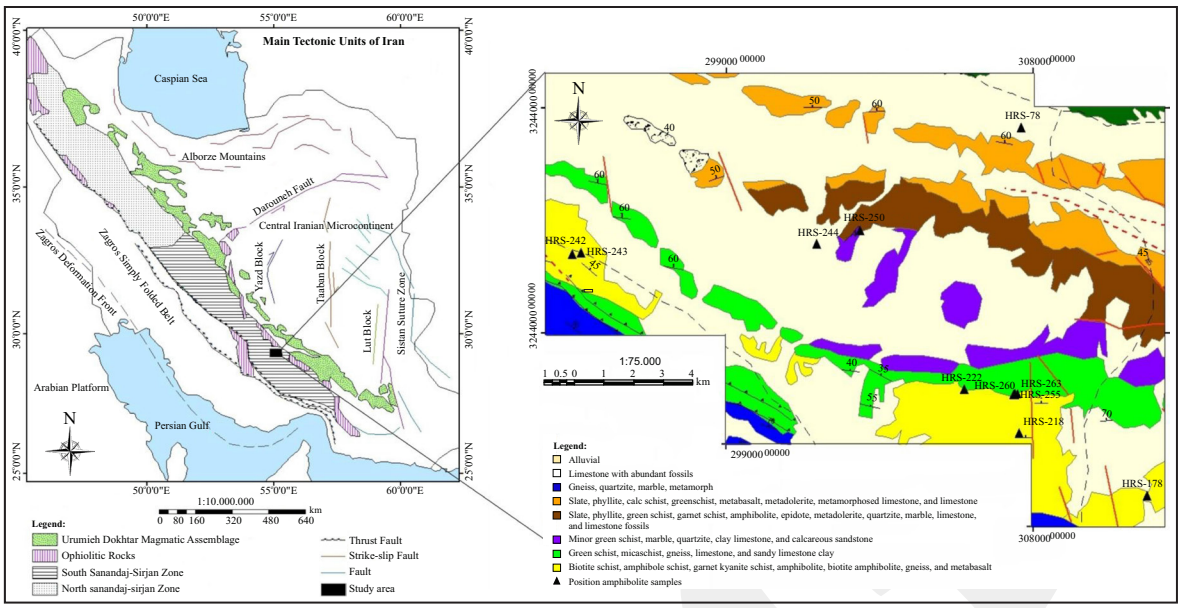

Figure 1. Distribution of the amphibolite rocks in northwest of Golgohar Iron Mine on the geological map with respect to the tectonic units of Iran (from Şengor, 1990).

Figure 2. Field photographs of amphibolites in northwest of Golgohar Iron Mine; a-b: amphibolite with distinct deformation and with the isoclinal microfold. c-d: massive amphibolites.

occasionally (Figures 2a-b). Original igneous textures are preserved in some of the amphibolites which show weak lineation and appear mainly as massive amphibolite (Figures 2c-d).

Methods and Materials

More than three hundred samples from different rock types of the studied area were col-

lected during the field investigations. Forty-five thin sections were made from the amphibolite samples and four well-studied representative samples (HRS-218, HRS-222, HRS-255, and HRS-263) with lowest alteration (lowest plagioclase change to clay) were chosen for Electron Probe Microanalysis and Raman Spectroscopy.

Petrography

Based on microscopic studies, amphibolite is ortho-amphibolite (monocline amphibole) and is metamorphosed basic igneous rock. Mineralogical evidence confirming igneous protolith for the amphibolite includes lack of calcite, rare quartz, and relatively high content of ferromagnesian minerals (mainly amphibole). The mineral assemblage includes hornblende + plagioclase ± epidote ± rutile ± titanite. Coarse brown-green amphiboles among sericitized and interlocked plagioclases show granoblastic texture (Figures 3a, b, and c). Textural relations among hornblende, plagioclase, opaque minerals,and secondary chlorite can be

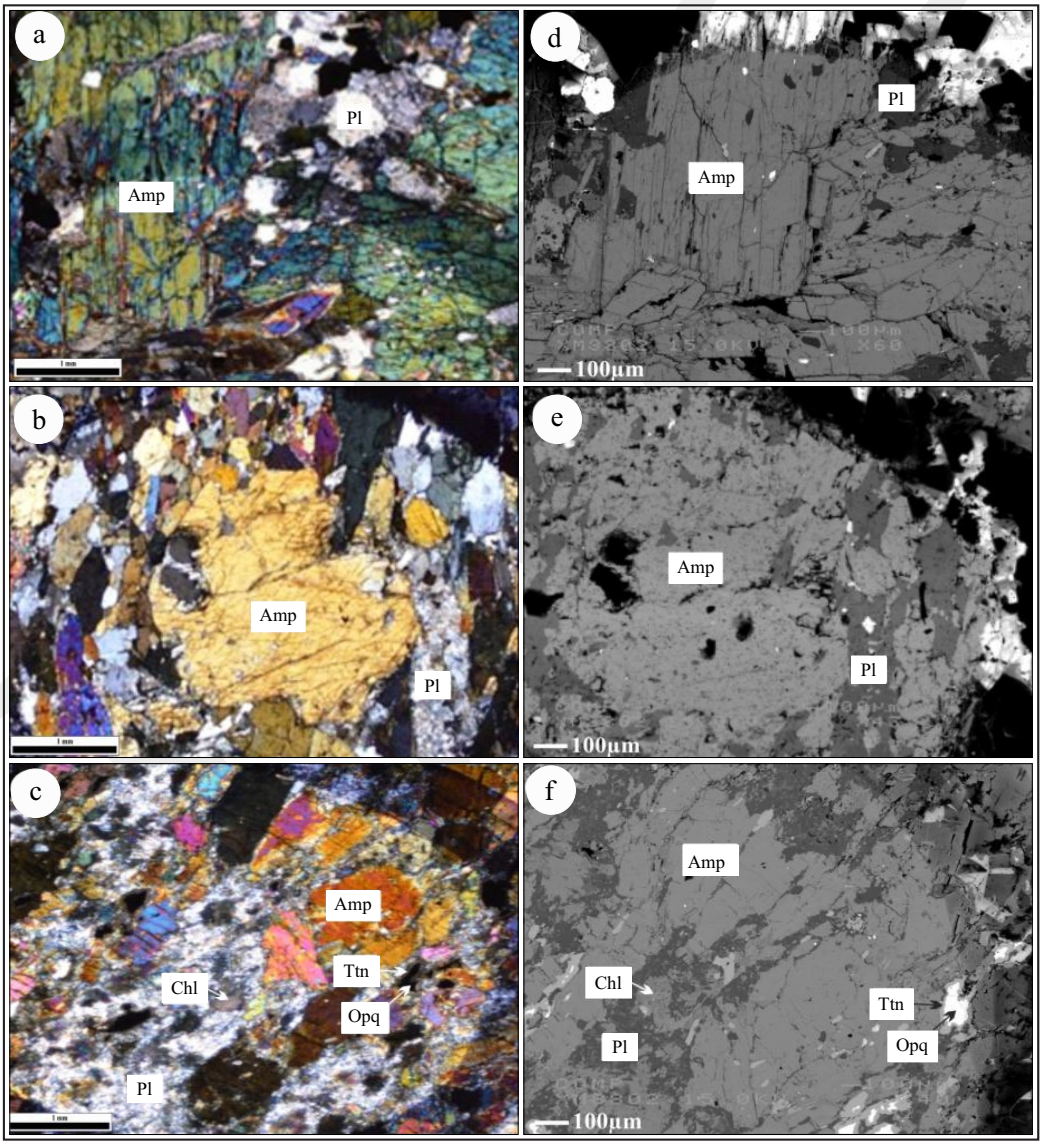

Figures 3a - c. Photomicrophotographs of amphibolite; sub-idioblastic amphiboles are interlocked in sericitized plagioclase, forming granoblastic texture; d - f: Back scattered electron images of amphibolite samples; d, e. Sub-idioblastic grains of amphibole with interdispersed plagioclase; f. Sub-idioblastic grains of amphibole in association with plagioclase, secondary chlorite, titanite, and opaque minerals. Abbreviation for minerals (Kretz, 1983): Amp: Amphibole, Pl: Plagioclase, Chl: Chlorite, Ttn: Titanite, Rt: Rutile, and Opq: Opaque minerals.

seen in back scattered electron images (Figures 3d, e,and f).

Electron Probe Microanalysis

Mineral chemical analyses were performed on polished thin sections using an automated JEOL JXA-8900 electron probe microanalyzer (EPMA) at the EMS Laboratory of Yamagata University in Japan with accelerating voltage of 15 kV, a beam current of 20 nA, a beam diameter of about 5 μm, detection limits of 0.05 wt.%, and a maximum 40-s counting interval. The data were processed by an online computer using the oxide ZAF in the XM-86 PAC programme of JEOL.

Raman Spectroscopy

Micro-Raman Spectroscopy on amphiboles was carried out by a JASCO micro-Raman Spectrometer (with a triple monochromator of 3 x 60 cm) in the Renishaw Raman Laboratory of Dr. Libowitzky in University of Vienna. The 488 nm line of an Ar laser was focused to an area of ~1 μm on the sample surface through a microscope (backscattering (180° geometry). The laser power was ~10 mW on the surface of the sample. The spectra were accumulated for 4-5 minutes to enhance the signal-to-noise ratio by using a multichannel detector (photodiode array). The wavenumber position and the full width at half maximum (FWHM) of the Raman peak were determined by carrying out a Lorentzian fitting of the spectrum. The wavenumber position of the Raman peak was calibrated using the 611 cm^{-1} emission lines in Raman shift of a Ne lamp. The spectral slit width was 3 cm, and the variation in room temperature was within 20.5 °C. More detailed analytical methods are described in Miyamoto and Ohsumi (1995).

Results

Amphibole Mineral Chemistry

The amphibole analyses are given in Table 1, which shows wide ranges in major element composition. Electron microprobe measurements were conducted on at least 3-8 points within each amphibole porphyroblast. In total, 42 of the 98 measured porphyroblasts have homogeneous compositions. Amphibole analysis gives the total sum ranging from 96 to 99.4 wt. %. Amphiboles vary from 43.00 to 47.43 wt.% in SiO_2, 10.07 to 15.15 wt.% in Al_2O_3, 8.84 to 11.61 wt.% in CaO, 9.72 to 16.55 wt.% in FeO, and 0.004 to 0.012 wt.% in TiO_2 contents.

Amphibole classification (after Leake *et al*., 2004) is based on the general chemical formula of $A_{0-1}B_2C_5{}^{V1}T^{1V}{}_8O_{22}(OH; F; Cl)_2$. Since the water and halogen contents of the amphiboles are not known, the amphibole formula is calculated to 23(O). The amphiboles are first classified based on the number of atoms per formula unit (apfu) of Ca and Na in the B site, *i.e.* $(Ca+Na)_B$. The recalculated amphibole analyses are classified into four groups on the occupancy of the B sites:

1. When $(Ca+Na)_B$ is <1.00 and the sum of L-type ions $(Mg, Fe, Mn, Li)_B$is ≥ 1.00, then the amphibole is a member of the magnesium ±iron±manganese±lithium group. This group is named as the iron±magnesium±manganese in the IMA (1978) nomenclature scheme.
2. When $(Ca)_B$ is ≥ 1.50,$(Ca+Na)_B$≥1.00 and Na_B<0.50 apfu, then the amphibole is a member of the calcic group.
3. When $(Ca+Na)_B$ is ≥ 1.00 and Na_B is in the range of 0.50 to 1.50, then the amphibole is a member of the sodic±calcic group.
4. When Na_B ≥ 1.50, then the amphibole is a member of the sodic group. The previous name of this group is called as the alkali group by the IMA (1978) scheme.

In this study,the classification parameters of $Ca+Na_B$ and Na_B have been used to separate four amphibole analyses onto each amphibole groups. The given diagram is harmonious with the binary amphibole plot by Mogessie *et al*. (1990). Following the primary divisions at Na_B< 0.50 and Na_B ≥ 1.50 between the calcic, sodic±calcic and sodic amphiboles, the binary $Ca+Na_B$ *vs*. Na_B group classification diagram (Figure 4) is

Table 1. Representative Microprobe Analysis of Amphibole Minerals from Northwest of Golgohar Iron Mine, Sirjan, Iran

Sample	HRS-218																				
Analysis	**2-1**	**2-2**	**2-3**	**2-5**	**2-6**	**2-7**	**2-2-1**	**2-2-2**	**2-2-4**	**3-2-2**	**3-2-3**	**3-2-4**	**3-3-1**	**3-3-3**	**3-3-4**	**3-1-1**	**3-1-2**	**3-1-4**	**3-1-6**	**5-1-1**	**5-1-4**
SiO_2	45.10	45.74	45.57	45.10	45.65	45.84	45.53	45.43	45.66	45.22	45.94	45.89	46.01	47.43	44.99	45.61	45.94	45.63	45.96	45.03	45.75
TiO_2	0.67	0.68	0.63	0.47	0.52	0.57	0.64	0.67	0.34	0.62	0.66	0.62	0.66	0.45	0.55	0.53	0.61	0.56	0.54	0.56	0.66
Al_2O_3	12.94	12.98	12.54	12.15	13.39	13.18	13.18	13.16	12.89	13.11	12.66	13.13	13.16	10.07	13.24	13.08	12.91	12.55	13.12	13.29	13.70
FeO	15.11	14.96	15.38	16.55	15.25	14.57	14.40	15.18	14.65	15.27	15.88	14.94	15.11	15.35	15.13	14.30	14.71	14.57	15.04	15.55	14.07
MnO	0.36	0.44	0.48	0.33	0.42	0.37	0.42	0.38	0.45	0.45	0.40	0.49	0.44	0.30	0.34	0.34	0.39	0.51	0.35	0.30	0.30
MgO	11.61	11.38	11.32	9.89	11.14	11.24	11.08	11.30	11.32	11.34	11.32	11.39	11.47	12.30	10.81	10.78	11.43	11.39	10.81	11.32	11.07
CaO	10.31	10.26	10.22	11.06	10.31	10.26	10.35	10.14	10.63	10.37	10.20	10.17	10.43	11.09	10.52	10.96	10.40	10.69	10.51	10.50	10.64
Na_2O	1.99	2.19	2.08	1.91	2.18	2.06	2.23	2.27	1.71	1.63	1.64	1.70	1.64	1.33	1.78	1.59	1.53	1.68	1.46	1.58	1.66
K_2O	0.30	0.32	0.31	0.34	0.30	0.28	0.28	0.33	0.25	0.33	0.33	0.27	0.31	0.26	0.30	0.30	0.29	0.27	0.26	0.29	0.30
Cr_2O_3	0.08	0.09	0.08	0.07	0.00	0.08	0.08	0.00	0.09	0.00	0.07	0.11	0.00	0.08	0.15	0.06	0.13	0.14	0.02	0.00	0.07
Total	98.47	99.03	98.60	97.88	99.14	98.44	98.19	98.86	97.98	98.35	99.09	98.72	99.22	98.67	97.80	97.54	98.34	98.00	98.08	98.42	98.22
O	23	23	23	23	23	23	23	23	23	23	23	23	23	23	23	23	23	23	23	23	23
Si	6.43	6.50	6.51	6.61	6.48	6.54	6.54	6.47	6.55	6.45	6.50	6.50	6.49	6.77	6.49	6.60	6.54	6.55	6.58	6.42	6.54
Ti	0.07	0.07	0.07	0.05	0.06	0.06	0.07	0.07	0.04	0.07	0.07	0.07	0.07	0.05	0.06	0.06	0.07	0.06	0.06	0.06	0.07
Al	2.17	2.18	2.11	2.10	2.24	2.22	2.23	2.21	2.18	2.20	2.11	2.19	2.19	1.69	2.25	2.23	2.16	2.12	2.21	2.23	2.31
Fe^{3+}	1.06	0.88	0.97	0.49	0.89	0.82	0.69	0.93	0.86	1.09	1.15	1.07	1.03	0.86	0.84	0.54	0.98	0.83	0.83	1.12	0.69
Fe^{2+}	0.75	0.89	0.87	1.54	0.92	0.92	1.04	0.88	0.89	0.73	0.73	0.70	0.75	0.97	0.98	1.19	0.77	0.92	0.97	0.73	0.99
Mn	0.04	0.05	0.06	0.04	0.05	0.04	0.05	0.05	0.06	0.05	0.05	0.06	0.05	0.04	0.04	0.04	0.05	0.06	0.04	0.04	0.04
Mg	2.47	2.41	2.41	2.16	2.36	2.39	2.37	2.40	2.42	2.41	2.39	2.40	2.41	2.62	2.32	2.33	2.42	2.44	2.30	2.40	2.36
Ca	1.58	1.56	1.56	1.74	1.57	1.57	1.59	1.55	1.63	1.58	1.55	1.54	1.58	1.69	1.62	1.70	1.58	1.64	1.61	1.60	1.63
Na	0.55	0.60	0.58	0.54	0.60	0.57	0.62	0.63	0.48	0.45	0.45	0.47	0.45	0.37	0.50	0.45	0.42	0.47	0.41	0.44	0.46
K	0.05	0.06	0.06	0.06	0.05	0.05	0.05	0.06	0.05	0.06	0.06	0.05	0.05	0.05	0.05	0.06	0.05	0.05	0.05	0.05	0.06
Cr	0.01	0.01	0.01	0.01	0.00	0.01	0.01	0.00	0.01	0.00	0.01	0.01	0.00	0.01	0.02	0.01	0.01	0.02	0.00	0.00	0.01
Total	15.18	15.22	15.19	15.34	15.22	15.19	15.26	15.23	15.15	15.10	15.05	15.06	15.08	15.11	15.18	15.20	15.06	15.16	15.07	15.09	15.14
Al(IV)	1.57	1.50	1.49	1.39	1.52	1.46	1.46	1.53	1.45	1.55	1.50	1.50	1.51	1.23	1.51	1.40	1.46	1.45	1.42	1.58	1.46
Al(VI)	0.61	0.68	0.62	0.71	0.73	0.76	0.77	0.68	0.72	0.65	0.61	0.69	0.68	0.46	0.74	0.84	0.70	0.67	0.79	0.65	0.85
C	5.00	5.00	5.00	5.00	5.00	5.00	5.00	5.00	5.00	5.00	5.00	5.00	5.00	5.00	5.00	5.00	5.00	5.00	5.00	5.00	5.00
B	2.00	2.00	2.00	2.00	2.00	2.00	2.00	2.00	2.00	2.00	1.99	2.00	2.00	2.00	2.00	2.00	2.00	2.00	2.00	2.00	2.00
A	0.18	0.22	0.19	0.34	0.22	0.19	0.26	0.23	0.15	0.10	0.06	0.06	0.08	0.11	0.18	0.20	0.06	0.16	0.07	0.09	0.14
$Mg/(Mg+Fe^{2+})$	0.77	0.73	0.74	0.58	0.72	0.72	0.69	0.73	0.73	0.77	0.77	0.77	0.76	0.73	0.70	0.66	0.76	0.73	0.70	0.77	0.70
$Fe^{2+}/Mg+Fe^{2+}$	0.23	0.27	0.26	0.42	0.28	0.28	0.31	0.27	0.27	0.23	0.23	0.23	0.24	0.27	0.30	0.34	0.24	0.27	0.30	0.23	0.30

Table 1. Continued...

Samples	HRS-222																HRS-255	HRS-263		
Analysis	**1-1**	**1-2**	**1-3**	**1-4**	**1-5**	**1-6**	**1-7**	**1-8**	**3-1-1**	**3-1-2**	**3-1-3**	**3-1-4**	**3-2-1**	**3-2-2**	**3-2-3**	**3-2-4**	**3-2-5**	**1-3**	**1-6**	**1-8**
SiO_2	44.22	43.00	44.09	44.56	44.10	44.99	44.57	45.12	44.19	44.87	44.27	44.80	44.80	44.34	44.56	44.83	44.16	46.79	45.89	47.17
TiO_2	0.93	0.88	0.75	0.80	0.85	0.66	0.80	0.69	0.81	0.79	1.04	0.77	0.80	0.78	0.79	0.82	0.92	0.47	0.56	0.52
Al_2O^3	14.09	14.38	13.92	14.03	13.42	13.23	13.36	13.75	13.82	13.73	14.09	13.93	13.58	14.12	13.40	13.57	14.32	13.29	15.15	14.83
FeO	14.35	15.30	14.85	15.29	14.15	14.98	14.71	15.32	14.24	15.16	15.38	14.74	15.81	15.97	15.30	15.57	15.93	12.89	11.39	9.72
MnO	0.26	0.23	0.24	0.17	0.16	0.20	0.24	0.21	0.16	0.22	0.23	0.14	0.18	0.25	0.26	0.10	0.24	0.31	0.19	0.24
MgO	10.30	10.33	10.22	10.24	10.56	10.85	10.66	10.69	10.59	10.83	10.56	10.97	10.28	10.34	10.68	10.49	10.14	14.15	13.42	13.35
CaO	10.69	10.92	11.23	11.47	11.53	11.33	11.48	11.28	11.19	11.00	11.19	11.32	11.40	11.00	11.61	11.05	11.17	8.84	10.13	10.23
Na_2O	1.86	1.80	1.80	1.69	1.72	1.67	1.66	1.72	1.82	1.72	1.90	1.69	1.88	1.89	1.63	1.67	1.80	1.80	2.15	1.89
K_2O	0.74	0.74	0.75	0.65	0.65	0.59	0.67	0.64	0.70	0.67	0.73	0.60	0.70	0.67	0.67	0.64	0.80	0.21	0.17	0.16
Cr_2O_3	0.02	0.07	0.08	0.01	0.02	0.07	0.00	0.07	0.03	0.00	0.03	0.01	0.14	0.05	0.03	0.00	0.04	0.16	0.11	0.15
Total	97.48	97.65	97.93	98.91	97.15	98.57	98.14	99.51	97.53	98.99	99.42	98.99	99.57	99.40	98.93	98.74	99.53	98.92	99.16	98.27
O	23	23	23	23	23	23	23	23	23	23	23	23	23	23	23	23	23	23	23	23
Si	6.45	6.28	6.44	6.44	6.49	6.50	6.49	6.46	6.46	6.43	6.36	6.43	6.46	6.36	6.44	6.46	6.35	6.40	6.35	6.57
Ti	0.10	0.10	0.08	0.09	0.09	0.07	0.09	0.07	0.09	0.09	0.11	0.08	0.09	0.08	0.09	0.09	0.10	0.05	0.06	0.05
Al	2.42	2.47	2.40	2.39	2.33	2.25	2.29	2.32	2.38	2.32	2.39	2.36	2.31	2.39	2.28	2.31	2.43	2.14	2.47	2.43
Fe^{3+}	0.47	0.71	0.38	0.40	0.24	0.52	0.39	0.55	0.37	0.66	0.56	0.56	0.42	0.68	0.48	0.59	0.58	1.84	1.09	0.72
Fe^{2+}	1.29	1.16	1.44	1.45	1.50	1.29	1.41	1.28	1.37	1.16	1.29	1.21	1.49	1.24	1.37	1.29	1.34	-0.37	0.23	0.41
Mn	0.03	0.03	0.03	0.02	0.02	0.02	0.03	0.03	0.02	0.03	0.03	0.02	0.02	0.03	0.03	0.01	0.03	0.04	0.02	0.03
Mg	2.24	2.25	2.23	2.21	2.32	2.34	2.31	2.28	2.31	2.31	2.26	2.35	2.21	2.21	2.30	2.25	2.17	2.88	2.77	2.77
Ca	1.67	1.71	1.76	1.78	1.82	1.75	1.79	1.73	1.75	1.69	1.72	1.74	1.76	1.69	1.80	1.71	1.72	1.30	1.50	1.52
Na	0.53	0.51	0.51	0.47	0.49	0.47	0.47	0.48	0.52	0.48	0.53	0.47	0.53	0.53	0.46	0.47	0.50	0.48	0.58	0.51
K	0.14	0.14	0.14	0.12	0.12	0.11	0.12	0.12	0.13	0.12	0.13	0.11	0.13	0.12	0.12	0.12	0.15	0.04	0.03	0.03
Cr	0.00	0.01	0.01	0.00	0.00	0.01	0.00	0.01	0.00	0.00	0.00	0.00	0.02	0.01	0.00	0.00	0.00	0.02	0.01	0.02
Total	15.33	15.36	15.41	15.37	15.43	15.33	15.38	15.33	15.40	15.29	15.38	15.32	15.41	15.34	15.38	15.29	15.37	14.81	15.11	15.06
Al(IV)	1.55	1.72	1.56	1.56	1.51	1.50	1.51	1.54	1.54	1.57	1.64	1.57	1.54	1.64	1.56	1.54	1.65	1.60	1.65	1.43
Al(VI)	0.87	0.75	0.84	0.84	0.82	0.75	0.78	0.78	0.84	0.76	0.75	0.78	0.76	0.75	0.73	0.77	0.78	0.54	0.82	1.00
C	5.00	5.00	5.00	5.00	5.00	5.00	5.00	5.00	5.00	5.00	5.00	5.00	5.00	5.00	5.00	5.00	5.00	5.00	5.00	5.00
B	2.00	2.00	2.00	2.00	2.00	2.00	2.00	2.00	2.00	2.00	2.00	2.00	2.00	2.00	2.00	2.00	2.00	1.77	2.00	2.00
A	0.33	0.36	0.41	0.37	0.43	0.33	0.38	0.33	0.40	0.29	0.38	0.32	0.41	0.34	0.38	0.29	0.37	0.04	0.11	0.06
$Mg/(Mg+Fe^{2+})$	0.64	0.66	0.61	0.60	0.61	0.64	0.62	0.64	0.63	0.67	0.64	0.66	0.60	0.64	0.63	0.64	0.62	1.15	0.92	0.87
$Fe^{2+}/Mg+Fe^{2+}$	0.36	0.34	0.39	0.40	0.39	0.36	0.38	0.36	0.37	0.33	0.36	0.34	0.40	0.36	0.37	0.36	0.38	-0.15	0.08	0.13

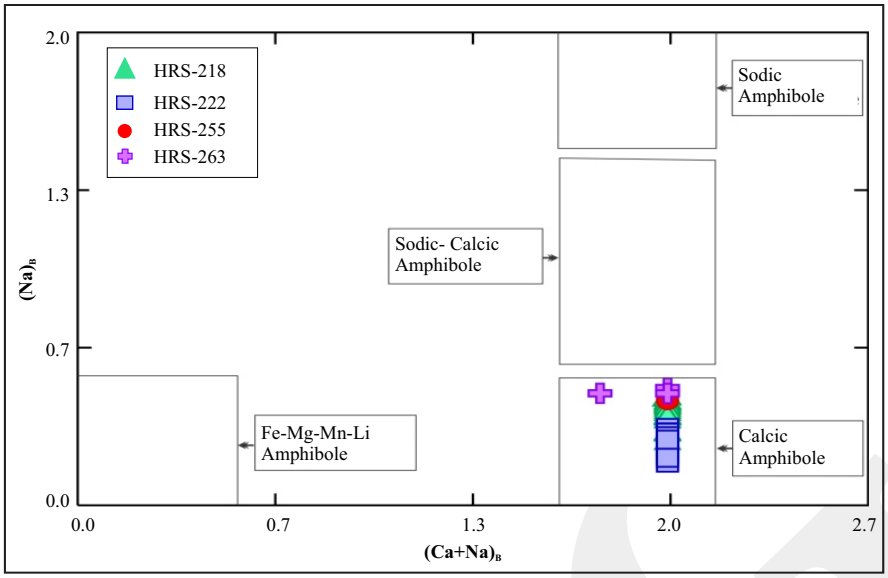

Figure 4. Plot of classification parameters on binary $(Ca+Na)_B$ *vs*. $(Na)_B$ diagram for amphibole group discrimination (Leake *et al*., 1997). All analyzed amphiboles are calcic amphiboles.

redrawn according to the IMA (1997) rules. According to this classification, all amphiboles in the amphibolites from northwest of Golgohar Iron Mine are plotted in the calcic amphibole field. The calcium amphiboles are defined by B $(Ca + \Sigma M^{2+})/\Sigma B \geq 0.75$, $BCa/\Sigma B \geq B\Sigma M^{2+}/\Sigma B$. These amphiboles typically have $(Ca+Na)B \geq 1.77$ with Si^{IV} between 6.27 and 6.76 apfu on the $Mg/(Mg+Fe^{2+})$ *vs*. Si classification diagram. The studied amphiboles predominantly range from tschermakite-hornblende to magnesio-hornblende in composition(Leake *et al*.,1997) (Figure 5). Amphiboles are characterized by $Mg^{\#}$ which is between 0.59 and 1.14, Si between 6.27 and 6.76 apfu (*e.g.* Leake, 1978).

The X_{Mg} values are in the range of 0.58-1.14, and positively correlated with the Si contents. The total aluminum content (Al_{tot}) shows a large variation from 1.73 to 2.55 apfuand is negatively correlated with the Si contents. Alkali (Na + K) contents range from 0.03 to 0.42 apfu and correlate negatively with Si, but positively with Al, as commonly observed in calcic amphiboles from calc-alkaline rocks (Féménias *et al*., 2006; Reichardt andWeinberg, 2012). The Ti contents show a similar trend and vary between 0.03 and 0.11 apfu (Figure 6). The analyzed amphiboles are compositionally homogenous throughout the grains, and Al contents between individual rims show a limited variation which suggests an equilibrium during crystal growth (Spear, 1981).

Raman Spectroscopy Results

Raman spectroscopy can distinguish between minerals which mineralogically and chemically are very close (Blaha and Rosasco, 1978; Wang *et al*., 1988a, 1988b; Lewis *et al*., 1996; Bard *et al*., 1997; Fornero *et al*., 2008).

The observed bands of Raman spectra can be ascribed only to the examined mineral without any interference from sample holders or embedding resin. All chemical bonds which change their polarizability after interaction with the laser incident beam are Raman-active (Fornero *et al*., 2008).

The orientation of the sample, regarding to the laser incident beam, indicates the intensity of the Raman spectra. The intensity of Raman bands does not indicate the amounts of the different chemical components since the orientation of the sampleis usually uncontrolled (Fornero *et al.,* 2008). Amphiboles have mostly complex chemical formulas with different electrovalence substitutions in equivalent crystallographic sites. Therefore, assigning bands in the spectral region $<600\ cm^{-1}$ is very difficult. Vibrational modes of

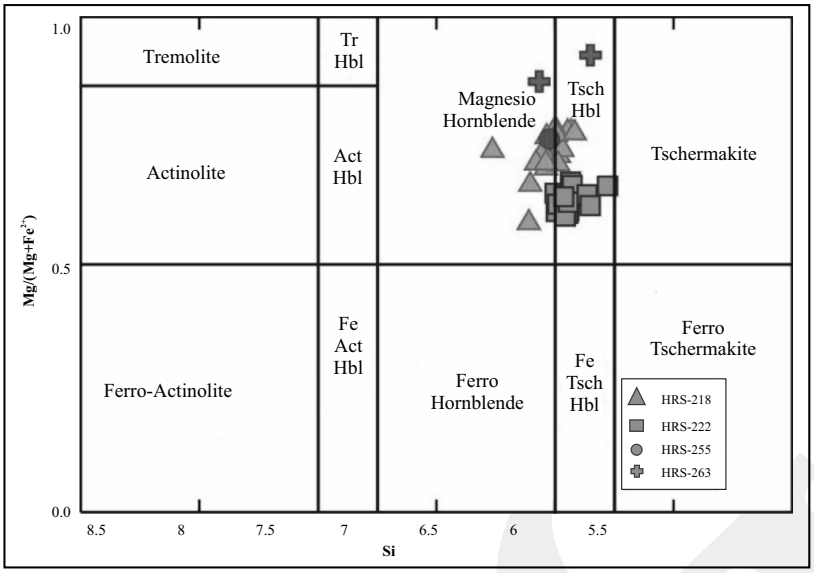

Figure 5. Composition of calcic amphiboles in the classification diagram (Leake *et al*., 1997).

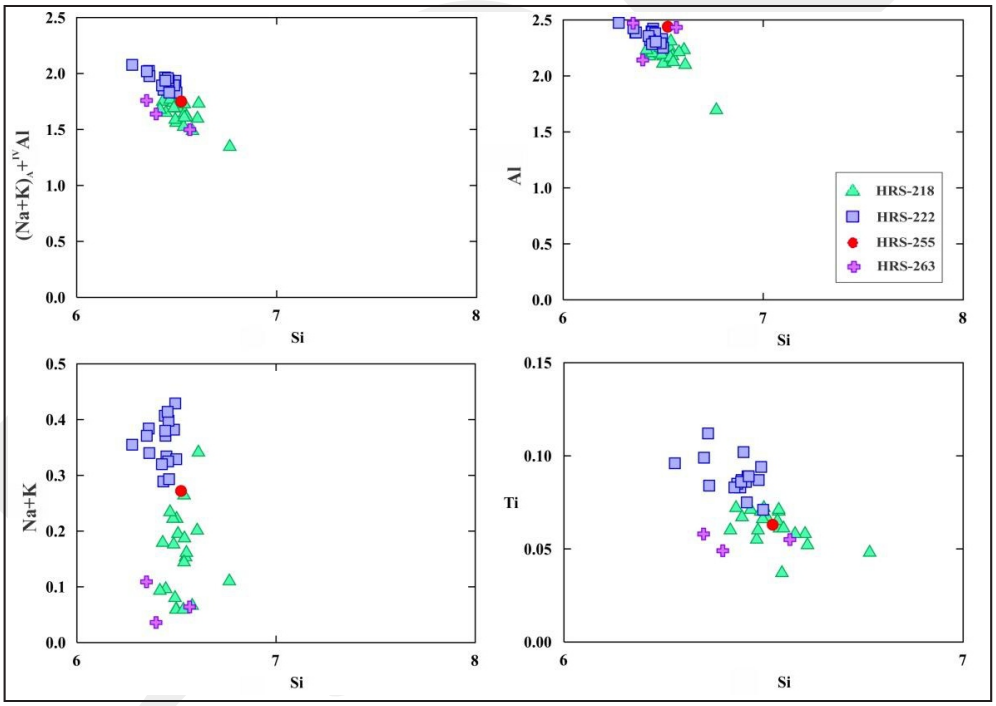

Figure 6. Compositional variations in amphiboles from northwest of Golgohar Iron Mine, Sirjan, Iran. Alkali (Na + K) contents correlate negatively with Si, positively with Al, as observed in calcic amphiboles, and Ti contents show a similar trend.

the cations occurring in octahedral or cubic coordination are active at this spectral region.This is due to bending modes of the SiO_4tetrahedra and the vibrations of the OH^- groups (Fornero *et al*., 2008).

In this work, only the Raman region corresponding to 100 - 1044 cm^{-1} was analyzed. The Raman spectra of amphiboles are shown in Figure 7. All of these spectra are very similar with small differences in the case of very low-intensity peaks (Figure 7). These amphiboles show broadly similar spectra to terrestrial tremolite. In contrast, terrestrial tremolite amphibole has quite different Raman spectra from amphiboles studied

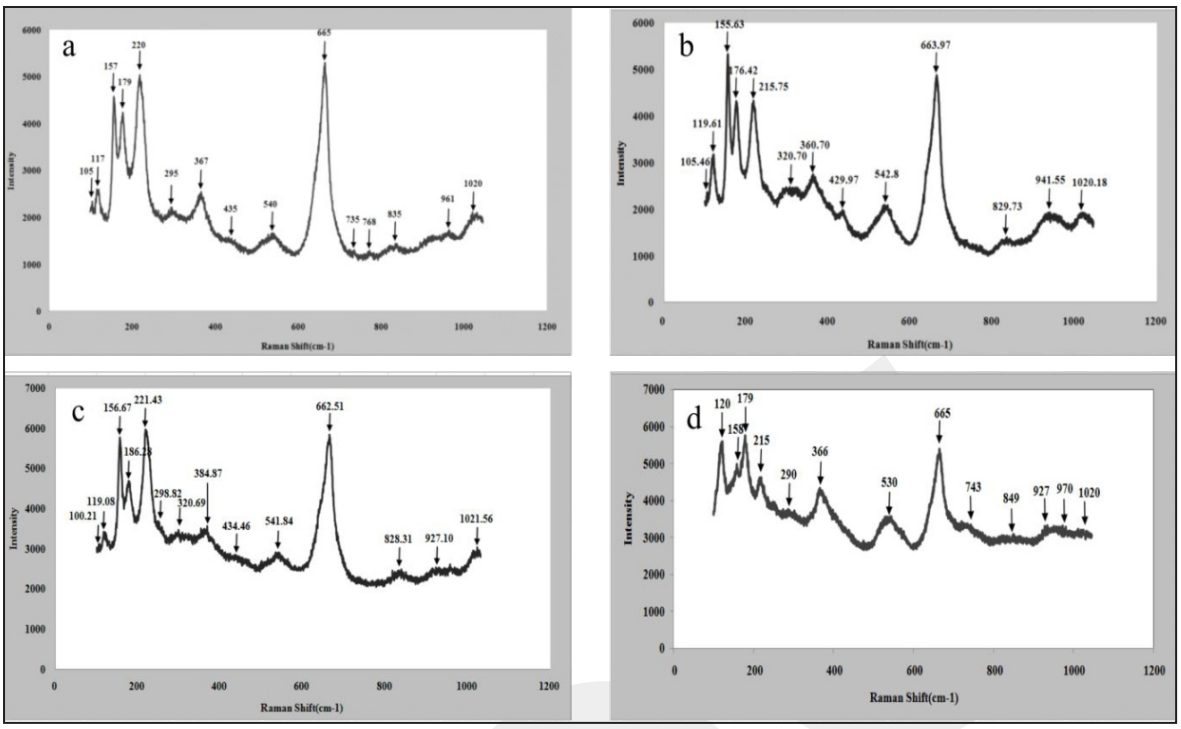

Figure 7. Micro-Raman spectra of the amphibole samples in the region of 100 - 1030cm^{-1}. (a,b). Amphibole sample HRS-218; (c,d).Amphibole sample HRS-222.

here (Figure 7), although these two amphiboles (HRS-218 and HRS-222) have the same space group and nearly identical cell parameters (space group: C2/m; cell parameters: a ≈ 9.85 A°, b ≈ 18.0-18.1 A°, c ≈ 5.3A°,p≈ 105A°) (Mikouchi and Miyamoto,2000). Studied amphiboles here have Raman peaks near 660 and 665 cm^{-1} which is similar to terrestrial tremolite that has the strongest peak at 667 cm^{-1} (Figure 7). Instead, the strong peak near 530 - 542 cm^{-1} in these amphiboles is very weak in tremolitic amphibole. Furthermore, the presence of strong peaks at the 210 - 300 cm^{-1}and 300 - 450 cm^{-1} region in the amphiboles is distinct from terrestrial tremolite (Figures 7 a - d).

Also, three peaks are present at 740, 920, and 1020 cm^{-1} region in our amphiboles (Figures 7 - d), which are at higher wave number than tremolite. These peaks (at 830, 940, and 970 cm^{-1}, respectively - see Figures7 - d) are part of O-Si-O symmetric stretching vibrations (νs). The bands at 1020 cm^{-1}, may be ascribed to the antisymmetric stretching vibrations (νas) of the Si-O_b-Si bridges. The bands at 730 - 740 cm^{-1} are debatable, given the fact that 740 cm^{-1} are the limit of νs. O-Si-O and νs Si-O_b-Si vibrations. The most intense bands, appearing at 650 cm^{-1}, are ascribed to the ν1 symmetric stretching modes (νs) of the Si-Ob-Si bridges. Considering bands in the 300 - 450 cm^{-1} spectral region, the assignments of the M-O vibrations are problematic; to see vibrations produced by Ca, Al, Mg, and/or Fe^{2+} cations. Nevertheless, the bands between 210 - 300 cm^{-1} are assigned to lattice modes. The following bands: 530, 538, and 540 cm^{-1} correspond to the deformation modes of Si_4O_{11}, with the observation that in this region there should be a liberational and translational vibration of the OH^- group.

Discussions

Mesozoic amphibolite rocks are exposed in the northwest of Golgohar Iron Mine at the southeast Sanandaj-Sirjan metamorphic belt, south-central Iran. Petrological studies show that amphibolites record medium to high-grade metamorphic facies

and are of ortho-amphibolite types. Plagioclase amphibolite, epidote amphibolite, and biotite amphibolite are the main ortho-amphibolite rock resulted in this regard. Amphibolites from this area were formed from igneous rocks with calc-alkaline protolith in a continental setting in Late Jurassic. Metamorphism changed the mafic rocks into amphibolite short after emplacement. Considering all these, Late Jurassic magmatism in southeast Sanandaj-Sirjan Zone triggered Neotethys ocean formation.

Both our amphiboles (tschermakite and magnesio-hornblende) and tremolite belong to calcic amphibole group (monoclinic amphibole). Generally, amphibole formula may be written as $A_{0\text{-}1}B_2C_5T_8O_{22}(OH,F)_2$ (*e.g*. Leake *et al*., 1997). In structural terms, the A, B, C, and T atoms are in A sites, M_4, M_1 +M_2 + M_3 and T (tetrahedral), respectively (*e.g*., Leake *et al*., 1997).

In the case of our amphiboles, which are tschermakite and magnesio-hornblende, the formula is given as $Ca_2(Mg_3AlFe^{3+})Si_6AI_2O_{22}(OH)_2$ and $Ca_2(Mg_4(Al,Fe^{3+}))Si_7AlO_{22}(OH)_2$. The formula of tremolite is $Ca_2Mg_5Si_8O_{22}(OH)_2$. Therefore, the difference in the Raman spectra between our amphiboles (tschermakite and magnesio-hornblende) and tremolite is more likely due to the difference of chemical compositions. Probably, the presence of the vacant A site, Al incorporation into M_1 + M_2 + M_3 sites, and into the T site produces different Raman spectra of tschermakite from tremolite.

Aluminum has an anionic radius, which is intermediate between the optimum radii for four-fold and six-fold co-ordinations, based on geometric packing (Hess, 1980). Al^{3+}can have the role of either a network-forming or a network-modifying cation in aluminosilicate formation. This is owing to the amphoteric nature of Al and radii between four-fold and six-fold coordinates.

Because of substitutions of Al^{3+} for Si^{4+} in tetrahedrons and Al^{3+}, Fe^{3+} for Mg^{2+}in octahedrons of the crystal lattice,it is supposed that the effect of the availability of a permanent positive charge can take place at the surface of amphiboles due to the substitutions of Al^{3+} for Si^{4+} in tetrahedrons and divalent cations for polyvalent cations in octahedrons of their crystal lattice.

Substitution of Al^{3+} for Si^{4+} may further increase the localization of these modes. It is probably the localized nature of the vas (T-O-T) modes that cause the vas (Si-O_b-Al) and vas (Si-O_b-Si) modes to appear at different frequencies.

Comparing Raman spectra for amphibole in amphibolite of the Golgohar area with spectrum for tremolite (Blaha and Rosasco, 1978; Lewis *et al*.,1996; Bard *et al*., 1997; Rinaudo *et al*., 2003, 2004;), the following observations can be made: (i) Two distinct bands at 602 and 1031 cm^{-1} on tremolite are the result of Si-O-Si bonding, and one board band is formed by one component lying at 1020 cm^{-1} on amphiboles studied here; (ii) Si-O-Si bridge v_1 symmetric stretching modes show vibration at slightly higher wave numbers than in tremolites (660, 665 cm^{-1}); (iii) narrow and well-defined band can be seen in the Raman spectrum for tremolite, while amphiboles studied here show more broad and convoluted bands. This can be attributed to a more complex chemical composition and frequent substitutions in the different structural sites of the amphiboles (*e.g*. Gianfagna and Oberti, 2001).

Conclusions

Microprobe analysis of amphiboles represents chemical compositions enriched in Al and Fe^{3+} that indicate types close to the tschermakite and magnesio-hornblende end-members in stoichiometry.

The presence of weak Raman bands corresponding to vas (Si-O-Si) modes, in addition to the sharp and well-defined vas (Si-O-Al) bands in the spectrum of crystalline amphiboles, implies a small degree of disorder in the substitution of Si-Al in the studied amphiboles. In these amphiboles, the presence of the half Al^{3+} ion in six-fold coordination enhances the intensities of the bands resulting from the nonbridging oxygens in the 900 - 1200 cm^{-1} region of the spectrum. However, the presence of the half Al^{3+} ions as tetrahedrally

coordinated network modifiers at the foursites in the structure increases the intensities of the symmetrical stretching bands of non-bridging oxygens.

There are not discriminable differences in Raman spectral peak pattern of amphiboles and terrestrial in low region wave number. While Raman peak patterns of tremolite have clearly different features *versus* tschermakite tremolite. This could be useful as a reliable tool for the same discrimination by Raman technique. The general differences between Raman spectral patterns of studied amphiboles with Raman peak patterns of introduced terrestrial tremolites are tied to the fact that the analyzed tschermakite and magnesio-hornblende amphiboles attributed to the complex chemical composition and considerable substitutions in the different tetrahedral, alkali, and more likely OH structural sites in the amphiboles of the studied area.

Acknowledgement

The authors would like to thank EMS Laboratory of Yamagata University and Renishaw Raman Laboratory of the University of Vienna for their help in microprobe and micro-Raman analyses. They are also grateful to the Geology Department of Shahid Bahonar University of Kerman for supporting this research

References

Aghanabati, A., 2006. *Geology of Iran*. 1st ed. Tehran, Iran. Geological Survey of Iran. p. 708. (in Persian).

Alavi, M., 1994. Tectonics of the Zagros orogenic belt of Iran: new data and interpretations. *Tectonophysics*, 229 (3-4), p.211-238. DOI: 10.1016/0040-1951(94)90030-2

Anderson, J.L. and Smith, D.R., 1995. The effects of temperature and fO_2 on the Al-in-hornblende barometer. *American Mineralogist*, 80 (5-6), p.549-559. DOI: 10.2138/am-1995-5-614

Bard, T., Yarwood J.,and Tylee B., 1997. Asbestos fiber identification by Raman microspectroscopy. *Journal of Raman Spectroscopy,* 28, p.803-809. DOI: 10.1002/(SICI)1097-4555(199710)28:10<803::AID-JRS151>3.0.CO;2-7

Berberian, M. and King, G.C., 1981. Towards a paleogeography and tectonic evolution of Iran. *Canadian Journal of Earth Sciences* 18, p.210 - 265. DOI: 10.1139/e81-019

Blaha, J.J. and Rosasco, G.J., 1978. Raman microprobe spectra of individual microcrystals and fibers of talc, tremolite, and related silicate minerals. *Analytical Chemistry,* 50, p.892-896. DOI: 10.1021/ac50029a018

Deer, W.A., Howie, R.A., and Zussman, J., 1992. *An introduction to the rock-forming minerals.* (2nd ed.): Longmans, Green and Co., London, 696pp.

Féménias, O., Mercier, J.C.C., Nkono, C., Diot, H., Berza, T., Tatu, M., and Demaiffe, D., 2006. Calcic amphibole growth and compositions in calc-alkaline magmas: evidence from the Motru Dike Swarm (Southern Carpathians, Romania). *American Mineralogist,* 91, p.73-81. DOI: 10.2138/am.2006.1869

Fornero,E., Allegrina, M., Rinaudo, C., Mazziotti -Tagliani, S., and Gianfagna, A., 2008. Micro-Raman spectroscopy applied on oriented crystals of fluoro-edeniteamphibole. *Periodico di Mineralogia,* 77, p.2-14, DOI: 10.2451/2008PM0008

Gianfagna, A. and Oberti, R., 2001. Fluoro-edenite from Biancavilla (Catania, Sicily, Italy): crystal chemistry of a new amphibole end-member. *American Mineralogist,* 86 (11-12), p.1489-1493. DOI: 10.2138/am-2001-11-1217

Hawthorne, F.C., Oberti, R., Harlow, G.E., Maresch, W.V., Martin, R.F., Schumacher, J.C., and Welch, M.D., 2012. Nomenclature of the amphibole supergroup. *American Mineralogist,* 97 (11-12), p.2031-2048. DOI: 10.2138/am.2012.4276

Hess, P.C., 1980. Polymerized model for silicate melts. *In*: R.B. Hargraves (eds.), *Physics of Magmatic Processes*, p.3-48.

Holland, T.J.B. and Blundy, J.D., 1994. Non-ideal interactions in calcic amphiboles and their bearing on amphibole plagioclase thermometry. *Contributions to Mineralogy and Petrology,* 116, p.433-447. DOI: 10.1007/BF00310910

Kretz, R., 1983. Symbols for rock-forming mineral. *American Mineralogist,* 68, p.227-279.

Leake, B.E., 1978. Nomenclature of amphiboles. *The Canadian Mineralogist,* 16, p.501-520.

Leake, B.E., Woolley, A.R., Arps, C.E., Birch, W.D., Gilbert, M.C., Grice, J.D., and Krivovichev, V.G.,1997. Nomenclature of amphiboles; report of the subcommittee on amphiboles of the International Mineralogical Association. Commission on New Minerals and Mineral Names. *European Journal of Mineralogy,* 82, p.1019-1037. DOI: 10.1127/ejm/9/3/0623

Leake, B.E., Woolley, A.R., Birch, W.D., Burke, E.A., Ferraris, G., Grice, J.D., and Schumacher, J.C., 2004. Nomenclature of amphiboles: additions and revisions to the International Mineralogical Association's amphibole nomenclature. *European Journal of Mineralogy,* 16 (1), p.209-215. DOI: 10.1127/0935-1221/2004/0016-0191

Lewis I.R., Chaffin N.C., Gunter M.E.,and Griffiths P.R., 1996. Vibrational spectroscopic studies of asbestos and comparison of suitability for remoteanalysis.Spectrochim. *Acta Part A; Molecular and Biomolecular Spectroscopy,* 52, p.315-328. DOI: 10.1016/0584-8539(95)01560-4

Mehdipour Ghazi, J. and Moazzen, M., 2015. Geodynamic evolution of the Sanandaj-Sirjan Zone, Zagros Orogen, Iran. *Turkish Journal of Earth Sciences,* 24, p.513-528, DOI: 10.3906/yer-1404-12

Mikouchi, T. and Miyamoto, M., 2000. Micro Raman spectroscopy of amphiboles and pyroxenes in the Martian meteorites. Zagami and Lewis Cliff 88516, *Meteoritic and Planetary Science,* 35, p.155-159. DOI: 10.1111/j.1945-5100.2000.tb01982.x

Miyamoto, M. and Ohsumi, K., 1995. Micro-Raman spectroscopy of olivines in L6 chondrites:evaluation of the degree of shock. *Geophysical Research Letters,* 22, p.437-440. DOI: 10.1029/94GL03281

Mogessie, A., Tessadri, R., and Veltman, C.B., 1990. EMPAMPH A Hypercard program to determine the name of an amphibole from electron microprobe analysis according to the International Mineralogical Association scheme. *Computers and Geosciences,* 16 (3), p.309-313. DO: 10.1016/0098-3004(90)90066-3

Mohajjel, M. and Fergusson, C., 2000. Dextral transpression in Late Cretaceous continental collision Zone, western Iran. *Journal of Structural Geology,* 22, p.1125-1139. DOI: 10.1016/S0191-8141(00)00023-7

Reichardt, H. and Weinberg, R.F., 2012. Hornblende chemistry in meta-and diatexitesand its retention in the source of leucogranites: an example from the Karakoram Shear Zone, NW India. *Journal of Petrology,* 53, p.1287-1318. DOI: 10.1093/petrology/egs017

Ricou, L.E., 1994. Tethys reconstructed: plates, continental fragments and their boundaries since 260 Ma. from Central America to Southeastern Asia. *Geodynamica Acta,* 7, p.169-218. DOI: 10.1080/09853111.1994.11105266

Rinaudo, C., Gastaldi, D., and Belluso, E., 2003. La spetroscopia Raman: tecnica di identificazionerapida di fibre di asbesto. *Siti Contaminati,* 2, p.116-120.

Rinaudo, C., Belluso, E., and Gastaldi, D., 2004. Assessment of the use of Raman spectroscopy for the determination of amphibole asbestos. *Mineralogical Magazine,* 68, p.455-465. DOI: 10.1180/0026461046830197

Rock, N.M.S. and Leake, B.E., 1984. The International Mineralogical Association amphibole nomenclature scheme: computerization and its consequences. *Mineralogical Magazine,* 48 (347), p.211-227. DOI: 10.1180/minmag.1984.048.347.05

Şengôr, A.M.C., 1990. A new model for the Late Paleozoic - Mesozoic tectonic evolution of Iran and implications for Oman. *In*: Robertson, A.H.F., Searle, M.P., and Ries, A.C. (eds.), *The Geology and Tectonics of the Oman region*, *Special Publication,* 49, Geological Society, London, p.797-831. DOI: 10.1144/GSL.SP.1992.049.01.49

Spear, F.S., 1981. Amphibole-plagioclase equilibria: an empirical model for the relation albite + tremolite= edenite + 4quartz.*Contribution to Mineralogy and Petrology,* 77, p.355-364. DOI: 10.1007/BF00371564

Stöcklin, J., 1968. Structural history and tectonics of Iran: a review. *AAPG Bulletin,* 52, p.1229-1258. DOI: 10.1306/5d25c4a5-16c1-11d7-8645000102c1865d

Tiepolo, M., Oberti, R., Zanetti, A., Vannucci, R., and Foley, S.F., 2007. Trace-element partitioning between amphibole and silicate melt. *Review in Mineralogy and Geochemistry,* 67, p.417-452. DOI: 10.2138/rmg.2007.67.11

Wang A., Dhamelincourt P., and Turrell, G., 1988a. Raman Microspectroscopic Study of the Cation Distribution in Amphibole. *Applied Spectroscopy,* 42, p.1441-1450. DOI: 10.1366/0003702884429490

Wang, A., Dhamelincourt P., and Turrell G., 1988b. Infrared and Low-Temperature Micro-Raman Spectra of the OH Stretching Vibrations in Cummingtonite. *Applied Spectroscopy,* 42, p.1451-1458. DOI: 10.1366/0003702884429526